Reduction in β^- decay half-lives of highly ionized fission products

Arkabrata Gupta[1,*], *Tripti* Biswas[2], *Chirashree* Lahiri[3], and *S.* Sarkar[4]

[1]Department of Basic Science and Humanities, Institute of Engineering and Management, University of Engineering and Management, Kolkata - 700160, India.
[2]Department of Physics, Acharya Prafulla Chandra College, New Barrackpore, Kolkata-700134, India
[3]Department of Physics, Surendranath Evening College, 24/2 M. G. Road, Kolkata-700009, India.
[4]Department of Physics, Indian Institute of Engineering Science and Technology, Shibpur, Howrah -711103 India.

Abstract. We calculate the rates of β^- decay of highly ionized long-lived and medium-lived fission products (LLFPs, MLFPs). These elements, produced as residues of nuclear fission in reactors, exhibit high radioactivity and prolonged half-lives, making them hazardous to the environment. To address this issue of nuclear waste management, we theoretically investigate the effects of β^- decay in highly ionized atoms. In the context of bare and highly ionized atoms, the presence of available phase space facilitates the generation of an electron within an unoccupied atomic orbital, a new channel of β^- decay i.e., the decay to the atomic bound state, opens along with the usual continuum state decay. As a result, the total β^- decay rate increases, significantly reducing the half-lives of the atoms, when they are made highly ionized or bare. In this work, we have calculated the total β^- decay half-lives in the case of highly ionized LLFPs (^{79}Se, ^{93}Zr, ^{99}Tc) and MLFPs (^{137}Cs, ^{151}Sm, ^{121}Sn, ^{147}Pm, ^{125}Sb, ^{155}Eu, ^{113}Cd), taking the contribution of both, the decay from continuum and bound states. Our calculations show that there will be a noticeable reduction in the half-life of the considered nuclei for highly ionized atomic configurations.

1 Introduction

The nuclear β^- decay refers to the process in which a neutron is converted into a proton along with the production of an electron and an electronic antineutrino, into the continuum states [1, 2]. Nonetheless, in the case of highly ionized and bare atoms, β^- decay to the continuum state is not the only available pathway, and the decay process exhibits distinct characteristics. In these highly ionized atoms, there remains a high probability for the emitted electron (during β^- decay) to be captured by one of the vacant atomic orbitals of the daughter atoms, leading to a new channel of β^- decay, apart from continuum state β^- decay, known as bound state β^- decay [3]. The bound state β^- decay can be understood as the time reversal of the electron capture process. In neutral atoms, the capacity of the phase space to accommodate the emitted electron is minimal. As we go on ionizing these atoms more lepton phase space becomes available for the considered atoms, and the new channel of β^- decay opens. This may lead to a significant decrement in the half-lives of the considered atoms.

*e-mail: arkabratagupta@gmail.com

This new channel of β^- decay was first predicted in 1947 by Daudel and collaborators [4] and since then, few theoretical studies have been conducted. Some of the major theoretical studies were made between 1960 and 1980, by various groups including Bachall [5] and Takahashi and collaborators [6, 7]. The research conducted in this domain has primarily concentrated on continuum and bound state β decay in neutrons, tritium, and fully ionized or bare heavy atoms. The inaugural experimental investigation was carried out in 1992 by Jung *et al.* [8], who documented the bound state β^- decay of the bare ^{163}Dy atom. This study utilized a storage ring to maintain the fully ionized parent atom. Soon, bound state β^- decay of fully ionized ^{187}Re, was studied by Bosch *et al.* [9], which helped in the calibration of ^{187}Re - ^{187}Os Chronometer.

Recent theoretical investigations into bound state β^- decay conducted by Gupta, Lahiri, and Sarkar [3, 10], have separately assessed the β^- decay rates for both continuum and bound states in stellar and terrestrial environments. Additionally, Singh Sidhu [11] has undertaken recent experimental research on the β^- decay of bare atoms, which encompasses an examination of the bound state β^- decay of the bare ^{205}Tl atom. Also, a recent study has been made on bare atom β^- decay of LLFPs, taking into account the temperature density dependence, by K. Volanis *et. al.* [12].

In nuclear power plants, the nuclear fuel left from reactors at the end of the nuclear reaction is not reprocessed but is disposed of as spent nuclear fuel (SNF) instead. This material is highly radioactive and contains certain elements that take an exceedingly long time to decay naturally, making them harmful to the environment. The SNF along with residual Uranium and Plutonium fuel, contains fission products which are classified based on their half-life values. the Fission products are classified as Medium-lived fission products (MLFPs) and Long-lived fission products (LLFPs) [13–16].

A radioactive element is classified as long-lived if its radioactive half-life is beyond 30 years to 100 years, while a medium-lived fission product has its half-life within the 30-year to 100-year range, which may vary to some extent [15]. It has been observed earlier that the half-life reduces significantly for atoms in their bare atomic configuration, while they undergo bound state β^- decay transitions [3]; based on this particular observation we have aimed to theoretically evaluate the changes in the decay rate and the half-lives of the considered fission products (FPs), for their three different highly ionized configuration of bare atomic state, H-like atomic state and He-like atomic state. This work can become useful in addressing the issue of nuclear waste management by attempting to reduce the half-lives of these harmful fission products and hence reducing their effects on the environment. In this work we have considered few of the major long-lived fission products (LLFPs) - ^{79}Se, ^{99}Tc, and ^{93}Zr. Along with LLFPs we have also considered the major medium-lived fission products (MLFPs) - ^{155}Eu, ^{113}Cd, ^{137}Cs, ^{121}Sn, ^{151}Sm, ^{147}Pm and ^{125}Sb [15, 16]. For these fission products, we have evaluated decay rates for different ionized states (He-like, H-like and bare atomic state) and compared the decay rates to determine the configuration with the highest decay rate. We have observed the variation in decay rates (i.e. half-life) with ionization states.

This paper is organized as follows, section [2] contains the methodology, which includes the working processes, the framework, and the background of the calculations made. The contribution of the atomic screening effect in highly ionized atoms and how it has been incorporated in the existing calculations are also discussed in this section. Next, the results of our study are discussed elaborately in section [3]. Finally, the conclusion of our work is described in section [4].

2 Methodology

This section outlines the formalism and steps for calculating decay rates and half-lives of selected fission products in highly ionized and bare atom configurations. Fission products are chosen from prior studies [15, 16], with relevant data sourced from modern experimental databases [17, 18]. Lepton phase volumes for bound and continuum state decays are calculated to compute the net decay rate ($\lambda_{\rm net}$) for highly ionized configurations. Calculations are restricted to allowed and first-forbidden transitions, as higher-order forbidden transitions contribute negligibly.

2.1 β^- decay rate in highly ionized atoms

The transition rates (in $\sec^{-1}$) for allowed transitions, nonunique first-forbidden transitions, and unique first-forbidden transitions, presented as a, nu and u respectively, are given as: [3, 6, 7, 19]

$$\lambda = [\ln 2/f_0 t](f_m^*), \tag{1}$$

for m = a (allowed), nu (nonunique) transitions. And

$$\lambda = [\ln 2/f_1 t](f_m^*), \tag{2}$$

for m = u (unique) transition. In this context, t represents the partial half-life associated with the specific β^- decay process. It is evaluated using the neutral atom half-life and the branching corresponding to the particular transition. The f_m^* is the Lepton phase volume. The functions f_x or g_x denote the larger component of the electron radial wave function. These functions are computed at a nuclear distance R corresponding to the daughter for the orbital x. The evaluation of f_x or g_x is achieved through the solution of the Dirac radial wave equations [20]. In this work, we have utilized the FORTRAN package RADIAL and its modified version to evaluate the radial wave functions [21, 22].

The mathematical representation of the decay rate function for allowed as well as for non-unique first-forbidden β^- transitions is as follows:

$$f_0(Z, W_0) = \int_1^{W_0} \sqrt{(W^2-1)}W(W_0 - W)^2 F_0(Z, W)L_0\, dW, \tag{3}$$

and, for unique first forbidden transitions, it follows

$$f_1 = \int_1^{W_0} \sqrt{(W^2-1)}W(W_0 - W)^2 F_0(Z, W)[(W_0 - W)^2 L_0 + 9L_1]\, dW. \tag{4}$$

The lepton phase space volume f_m^* associated with the continuum state of β decay can be articulated as follows:

$$f^*_{(m=a,nu)}(continuum) = \int_1^{W_c} \sqrt{(W^2-1)}W(W_c - W)^2 F_0(Z, W)L_0\, dW, \tag{5}$$

and,

$$f^*_{(m=u)}(continuum) = \int_1^{W_c} \sqrt{(W^2-1)}W(W_c - W)^2 F_0(Z, W)L_0 \times [(W_c - W)^2 L_0 + 9L_1]\, dW. \tag{6}$$

Here,

$$W_c = \frac{Q_c}{m_e c^2} + 1 \tag{7}$$

denotes the maximum energy that can be imparted to the emitted β^- particle. The detailed forms of the parameters W_0, L_0, F_0, L_1 and F_1 are referenced from the Refs. [3, 7].
Here, for bare parent atoms,

$$Q_c = Q_n - [B_n(Z+1) - B_n(Z)]. \tag{8}$$

For H-like parent atom,

$$Q_c = Q_n - [B_n(Z+1) - B_n(Z)] + [B_{H-like}(Z+1) - B_{H-like}(Z)], \tag{9}$$

For He-like parent atom,

$$Q_c = Q_n - [B_n(Z+1) - B_n(Z)] + [B_{He-like}(Z+1) - B_{He-like}(Z)]. \tag{10}$$

The expression $[B_n(Z+1) - B_n(Z)]$ indicates the difference in binding energies between the parent atom and the daughter atom in their neutral configuration. The term $[B_{H-like}(Z+1) - B_{H-like}(Z)]$ represents the difference between the binding energies of the parent atom and daughter atom for their respective H-like configuration. Similarly, $[B_{He-like}(Z+1) - B_{He-like}(Z)]$ represents the difference between the binding energies of the parent and daughter atoms for their respective He-like configuration. These data are referred from [17, 18].

For Bound state β^- decay the lepton phase volume function takes the form

$$f^*_{(m=a,nu)}(bound) = \sum_x \sigma_x \left(\frac{\pi}{2}\right) [f_x \, or \, g_x]^2 b^2 \quad (\text{for } x = ns_{(1/2)}\, np_{(1/2)}), \tag{11}$$

and,

$$f^*_{(m=u)}(bound) = \sum_x \sigma_x \left(\frac{\pi}{2}\right) [f_x \, or \, g_x]^2 b^4 \quad (\text{for } x = ns_{(1/2)}\, np_{(1/2)}). \tag{12}$$

In this context, we choose σ_x=1 for the bare atom, which signifies the orbital vacancy. It varies accordingly with the atomic configuration of the parent atom.

And,

$$b = \frac{Q_b}{m_e c^2}, \tag{13}$$

where, for bare atoms,

$$Q_b = Q_n - [B_n(Z+1) - B_n(Z)] + B_{shell}(Z+1), \tag{14}$$

which can also be written in the form,

$$Q_b = Q_{c(bare)} + B_{H-like}(Z+1). \tag{15}$$

Similarly, for H-like parent,

$$Q_b = Q_{c(H-like)} + B_{He-like}(Z+1), \tag{16}$$

and, for He-like parent,

$$Q_b = Q_{c(He-like)} + B_{Li-like}(Z+1). \tag{17}$$

Here, we consider B_{shell} as the ionization energy corresponding to that shell. More clearly, $B_{H-like}(Z+1)$, $B_{He-like}(Z+1)$ and $B_{Li-like}(Z+1)$ represent the ionization energies of the particular shells that might capture the emitted electron in the bound state β^- decay of a bare, H-like and He-like parent atom respectively, giving rise to corresponding daughter atoms of H-like, He-like and Li-like configurations each, respectively [18].

The bound and continuum state decay rates (λ_b an λ_c respectively) of each β^- transition from a parent ground/isomeric state are evaluated and added up to get the total decay rate (λ_{tot}) of that transition. Finally, the total decay rate of all the possible transitions is summed up to get the net β^- decay rate (λ_{net}) of that particular parent nuclei. This net decay rate is used to evaluate the half-life of the highly ionized parent atom and then a comparison is taken with the corresponding neutral atom half-life for further analysis.

$$\lambda_{tot} = \lambda_b + \lambda_c, \tag{18}$$

$$\lambda_{net} = \sum \lambda_{tot}. \tag{19}$$

It must be clearly understood that calculations for all the parameters here, have been done separately for the three distinct levels of ionization (He-like, H-like and bare state), of the fission products considered in this work.

After the net decay rates (λ_{net}) are evaluated, corresponding half-lives can be obtained as

$$T_{1/2(\text{bare or H-like or He-like})} = \frac{ln(2)}{\lambda_{net}}, \tag{20}$$

The half-lives are evaluated separately for three different levels of ionization (He-like, H-like and bare state) and then compared separately for each ionization level, with the neutral atom half-lives (T_N) for further analysis.

The reduction factor (R) (i.e., the reduction in half-life) is evaluated by taking the ratio of the total decay rate for the atoms with highly ionized configuration, to the decay rate for neutral atom configuration of the same atom. This factor is evaluated for individual transitions as well as taking into all possible transitions from parent nuclei [3],

$$R = \frac{\lambda_{tot}}{\lambda_{neutral}}\ . \tag{21}$$

2.2 Atomic Screening

The screening effect or shielding effect refers to the phenomena where the electrons present in the outer orbitals of an atom, experience a reduced force of attraction by the nucleus due

to the presence of electrons in the inner orbitals [23]. This screening effect in turn affects the nuclear charge (Z) experienced by the emitted electron and the radial wave functions of that emitted electron.

In the case of the bound state β^- decay of the bare atoms, due to the absence of orbital electrons, screening effect is absent. However, we must incorporate the atomic screening effect in case of the bound state β^- decay for highly ionized atoms, to obtain the proper Dirac radial wave function of the emitted β particle.

In this work, we have considered highly ionized configurations (bare, H-like, and He-like) of the parent atoms. Based on Slater's work [24], we have evaluated the effective nuclear charge (Z_{eff}) for He-like and Li-like daughter atoms corresponding to H-like and He-like parent atoms, respectively. For an H-like parent, one electron occupies the 1s orbital in the parent atom, allowing the emitted β electron to occupy the 1s, 2s, 3s, or 4s orbitals, forming a daughter atom of He-like configuration. For a He-like parent, two electrons already occupy the 1s orbital, preventing further capture in this orbital, the emission of a β particle results in a daughter atom of Li-like configuration. Capture by p-orbitals is excluded due to their negligible radial wave functions. The Z_{eff} for these orbitals is evaluated as follows.

In case of H-like parent,

$$\text{for 1s} : Z_{eff} = Z - 0.3, \tag{22a}$$

$$\text{for 2s} : Z_{eff} = Z - 0.85, \tag{22b}$$

$$\text{for 3s} : Z_{eff} = Z - 1, \tag{22c}$$

$$\text{for 4s} : Z_{eff} = Z - 1. \tag{22d}$$

In case of He-like parent,

$$\text{for 2s} : Z_{eff} = Z - 1.7, \tag{23a}$$

$$\text{for 3s} : Z_{eff} = Z - 2, \tag{23b}$$

$$\text{for 4s} : Z_{eff} = Z - 2. \tag{23c}$$

These effective nuclear charge (Z_{eff}) values are used further, for the evaluation of the electron Dirac radial wave functions as discussed in the following section.

3 Results and discussions

We first examine how the lepton phase volume varies with the neutral atom Q-values (Q_n) for different ionization states. Subsequently, we examine the variation in the ratio of bound to continuum state decay rates (λ_b/λ_c) in relation to the neutral Q-values (Q_n) for various β^-transitions originating from the ground or isomeric state of the parent nucleus. We also investigate the net decay rates of highly ionized atoms (λ_{bare}, $\lambda_{\text{H-like}}$, $\lambda_{\text{He-like}}$) and compare these to the neutral atom decay rate (λ_{neutral}). These studies are carried out for three different ionization states (He-like, H-like, and bare atom) of the considered fission products.

3.1 The lepton phase volume

The β^- decay rate is directly dependent on the lepton phase volume. Variation of the lepton phase volume over different ionization states thus changes the decay rate. In the case of continuum state β^- decay, the main factor affecting the lepton phase volume for different ionization states is the β decay Q-value, due to its dependency on atomic binding energies as discussed in Sec. [2.1]. Whereas, in the case of bound state β^- decay the dependency arises due to several facts, such as Q-value, atomic screening which affects the radial component of Dirac wave function, and the occupancy probability.

In this work, we have calculated the electron Dirac radial wave function incorporating the screening effect, in case of H-like and He-like parent atoms. Our results show that, the effect of the atomic screening on the radial wave functions is small yet observable in these cases. For example, consider the case of the decay of ^{125}Sb. Figure [1] shows the variation of the radial wave functions of ^{125}Te (daughter atom of ^{125}Sb), with increasing level of ionization (He-like, H-like, and bare). It can be readily observed that the atomic screening has a small effect on the radial wave functions of the different orbitals. The overall nature of the radial wave functions of each considered orbital remains the same for different levels of ionization.

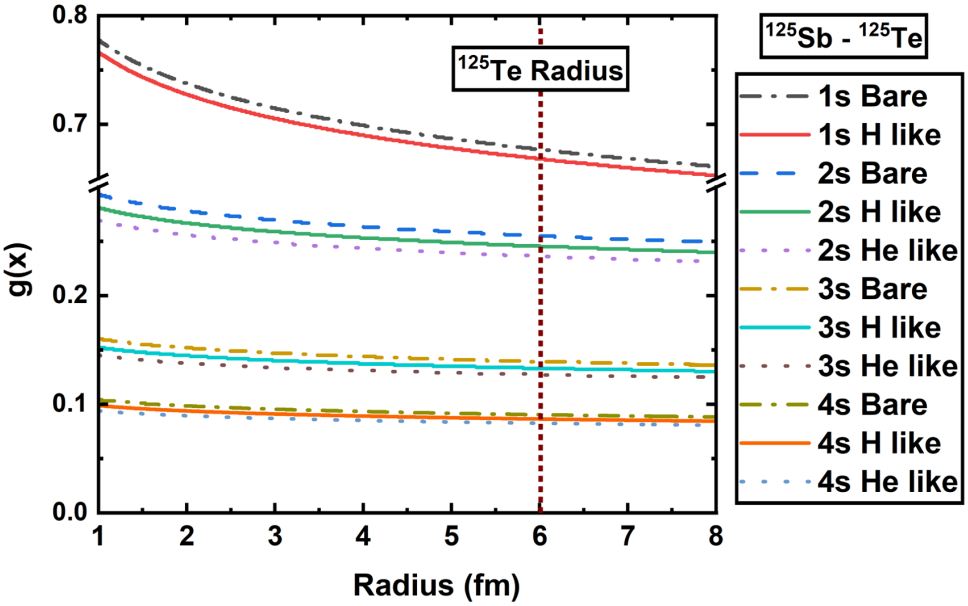

Figure 1. Variation of the radial wave functions of ^{125}Te for bare, H-like, and He-like configuration, corresponding to 1s, 2s, 3s, and 4s orbitals with the nuclear radius.

On the other hand, different ionization states lead to variations in electron vacancy (σ_x) in the atomic orbitals which in turn affects the lepton phase volume. Figure [2] represents the variation of the lepton phase volume of the different transitions of ^{125}Sb to its daughter, for its bare, H-like, and He-like configuration, with the neutral atom Q-value (Q_n). It can be observed that the increasing ionization (from he-like to bare) affects the lepton phase volume significantly. As the atom becomes highly ionized, the lepton phase volume increases. Hence, bound state decay probability rises. A bare atom has the maximum lepton phase space, resulting in the highest bound-state β^- decay probability and rate.

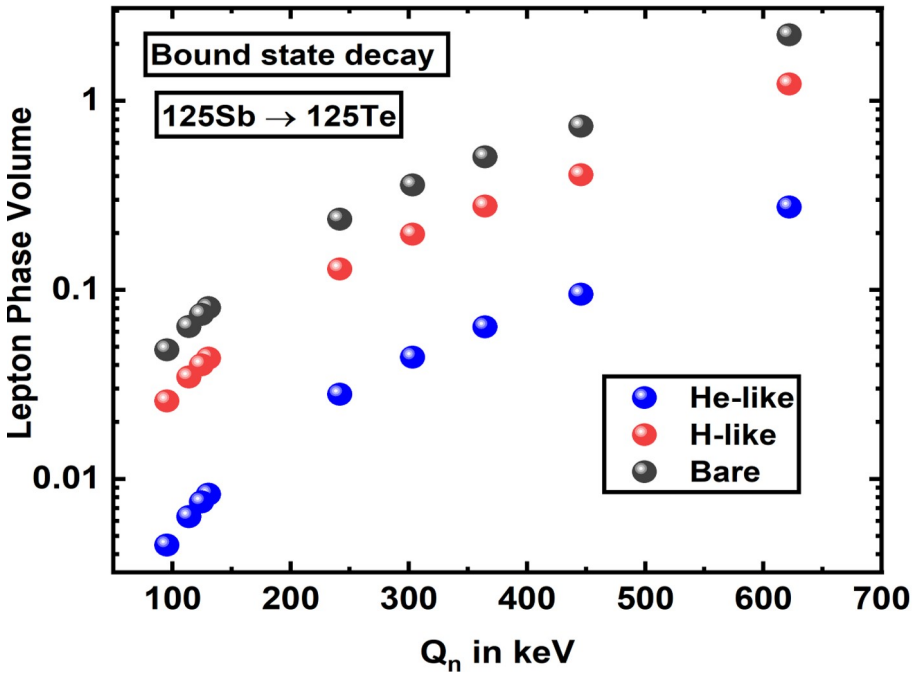

Figure 2. Variation of the bound state lepton phase volume along with the variation of neutral atom Q-value (Q_n), for different transitions of ^{125}Sb to its daughter atoms for its different highly ionized atomic configurations of bare atom, H-like atom and He-like atom.

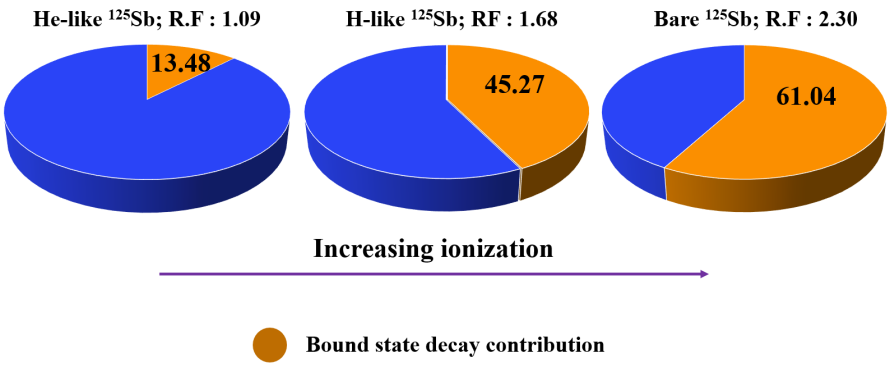

Figure 3. The contribution of the bound state β^- decay channel to the overall decay rate is analyzed for three distinct highly ionized states in the context of the β^- decay of ^{125}Sb. (He-like, H-like, and bare atom configuration) along with the corresponding reduction factors (R) for each ionized state.

Ionization affects the bound-state lepton phase space more significantly than the continuum state, owing to its dependence on multiple factors discussed earlier. The Figure [3] reflects the bound state decay rate contribution to the total decay rate in case of the decay of ^{125}Sb. It can be observed that the contribution of bound state increases, as the level of

ionization increases. The highest bound state decay rate contribution is observed for the bare atomic configuration.

3.2 The decay rate ratio between bound and continuum states

Figure 4 illustrates the relationship between the ratio of the decay rates of bound states (λ_b) to continuum states (λ_c) and the Q-value of neutral atoms. This analysis encompasses various transitions originating from the ground and isomeric states of four distinct fission products: ^{155}Eu, ^{147}Pm, ^{125}Sb, and ^{99}Tc. It can be observed that the ratio λ_b/λ_c increases with decreasing neutral atom Q-value Q_n, i.e., the bound state decay dominates for the transitions having lower Q_n value.

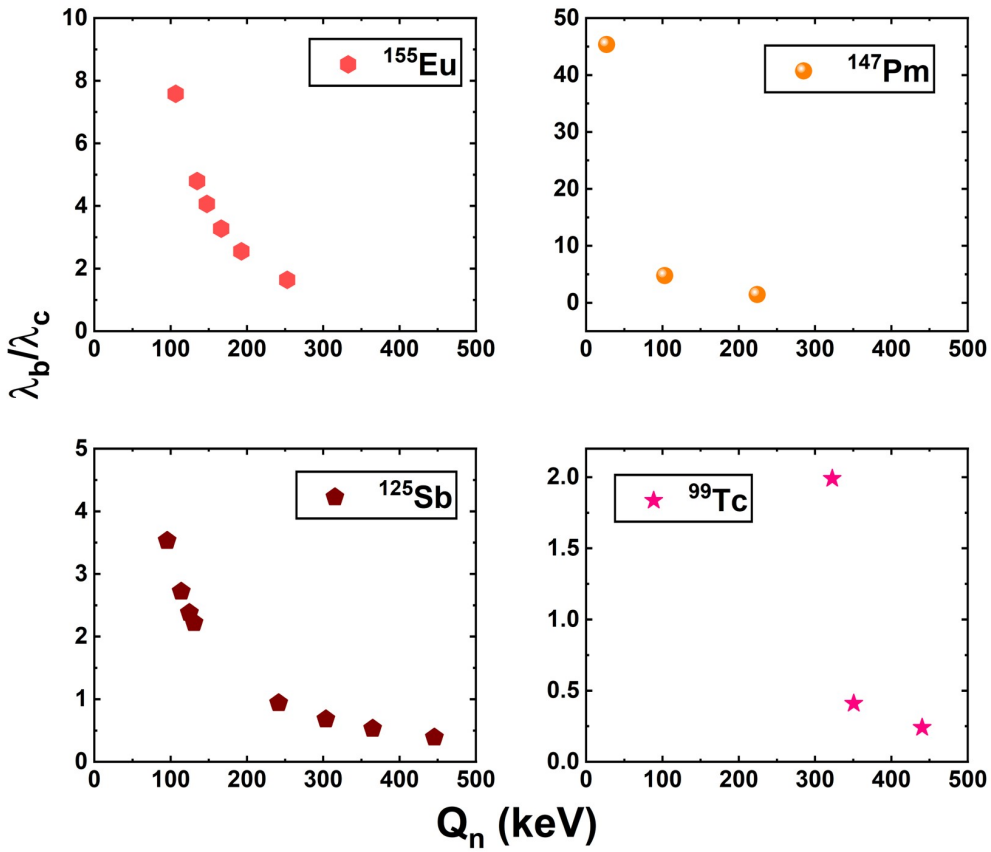

Figure 4. Variation of the bound to continuum state decay rate ratio ($\lambda_b : \lambda_c$), with the neutral atom Q-values (Q_n), for decay of ^{155}Eu, ^{147}Pm, ^{125}Sb and ^{99}Tc, in their bare atomic configuration.

3.3 Total decay rate

In the case of highly ionized atoms, the overall decay rate can be expressed as the aggregate of the decay rates associated with both bound states and continuum states ($\lambda_{tot} = \lambda_b + \lambda_c$).

As the bound state decay rate increases with the ionization state of the parent atom, the total decay rate also increases. Furthermore, since bound state decay dominates over continuum state decay for transitions with lower Q-values, the total decay rate rises more significantly, compared to the neutral atom decay rate for these transitions. Consequently, the partial half-life for each transition decreases (R) non-uniformly. Figure [5] illustrates the variation of the reduction factor (R) with the neutral atom Q-values for different transitions of ^{125}Sb to its daughter atom, across three highly ionized configurations (He-like, H-like, and bare).

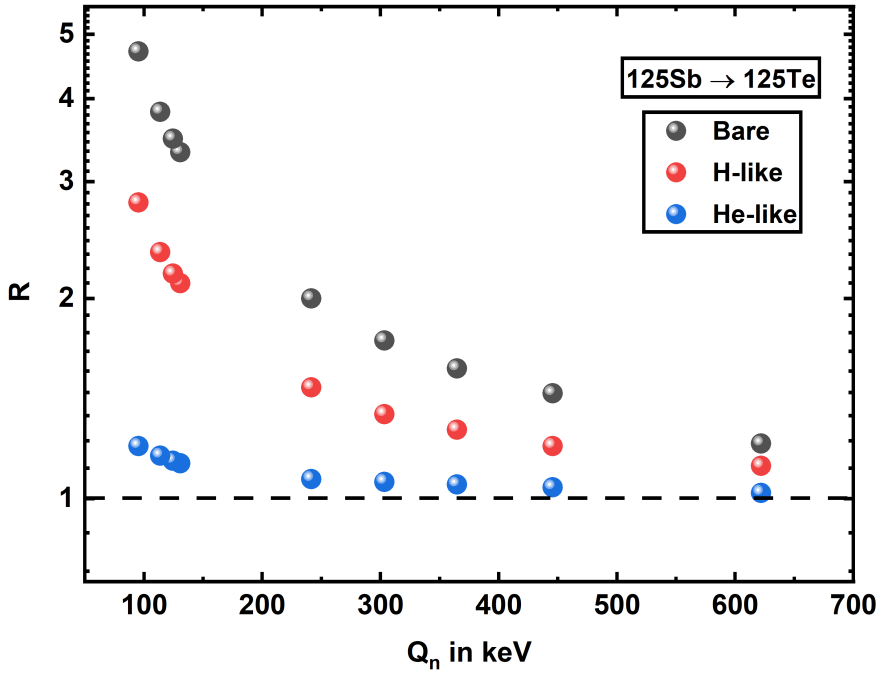

Figure 5. Variation of the reduction factor (R), with neutral atom Q-value (Q_n), for different transitions of ^{125}Sb to its daughter atoms for its bare, H-like and He-like atomic configurations.

The reduction factor (R) is consistently observed to remain above unity for all three highly ionized states (He-like, H-like, and bare). This indicates a definite decrease in partial half-lives (i.e., an increase in decay rates) for highly ionized atoms across different transitions. Although R exceeds 1 for all configurations, it is highest for the bare atom, which can be explained by the lepton phase volume discussed earlier.

In Figure [6], the variation of the ratio of bare atom decay rate to the neutral atom decay rate ($\lambda_{bare}/\lambda_{neutral}$) with neutral atom Q-value is shown for the decay of ^{155}Eu, ^{147}Pm, ^{125}Sb and ^{99}Tc. It can be observed that the $\lambda_{bare}/\lambda_{neutral}$ follows the same pattern as λ_b/λ_c, i.e., for the bare atom, the decay rate enhances more for the transitions having lower Q-values. Also, it is to be noted that the ratio is always greater than one, i.e., for all the transitions there must be an enhancement.

Finally, Table [1] summarises the total β^- decay half-lives of the fission products of interest for three ionized configurations and their respective reduction factors. It confirms that R always exceeds unity for highly ionized configurations, indicating a notable reduction in half-life, with the bare atom configuration showing the maximum reduction. Factors such as

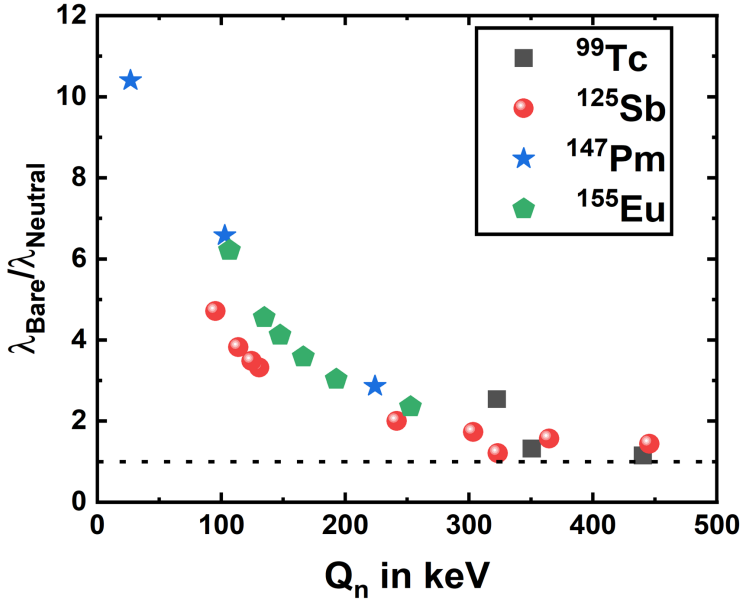

Figure 6. Variation of bare to neutral atom decay rate ratio ($\lambda_{bare} : \lambda_{neutral}$) with neutral atom Q-values (Q_n), for decay of ^{155}Eu, ^{147}Pm, ^{125}Sb and ^{99}Tc in their bare atomic configuration.

FP	$T_{1/2(N)}$ (yrs.) (NNDC [17])	$T_{1/2(He-like)}$ (yrs.)	R $_{He-like}$	$T_{1/2(H-like)}$ (yrs.)	R $_{H-like}$	$T_{1/2(bare)}$ (yrs.)	R $_{bare}$
^{79}Se	3.26×10^5	3.22×10^5	1.01	2.91×10^5	1.12	2.60×10^5	1.25
^{93}Zr	2.21×10^6	2.27×10^6	0.97	1.78×10^6	1.24	1.69×10^6	1.30
^{99}Tc	18.53	17.12	1.08	14.81	1.25	14.08	1.32
^{113}Cd	14.10	13.66	1.03	12.52	1.13	11.90	1.19
^{121}Sn	195.98	190.70	1.03	165.03	1.19	100.97	1.94
^{125}Sb	2.76	2.54	1.09	1.64	1.68	1.20	2.30
^{147}Pm	2.62	2.25	1.17	0.94	2.79	0.92	2.85
^{137}Cs	31.76	30.61	1.04	26.91	1.18	20.39	1.56
^{151}Sm	90.00	60.20	1.49	15.36	5.86	9.13	9.86
^{155}Eu	4.75	3.84	1.24	1.92	2.48	1.31	3.63

Table 1. Comparison of the neutral atom β^- decay half-life ($T_{1/2(N)}$) with the highly ionized atom half-life ($T_{1/2(bare)}$, $T_{1/2(H-like)}$, $T_{1/2(He-like)}$) of the different considered fission products along with their corresponding reduction factors (R_{bare}, R_{H-like}, $R_{He-like}$ respectively).

neutral atom Q-values and the type of β transitions (allowed or forbidden) influence the reduction factor. For this set of nuclei, the reduction factor ranges from 1.19 (for ^{113}Cd) to 9.86 (for ^{151}Sm). In the case of the long-lived fission products such as ^{79}Se and ^{93}Zr, the reduction in half-life does not have a significant impact. However, for medium-lived fission products,

such as ^{151}Sm (half-life reduces from 90 years to 9 years) and ^{155}Eu (half-life reduces from 4.7 years to 1.3 years), the reduction is impactful.

4 Conclusion

In conclusion, the higher the ionization of an atom, the greater the contribution of the bound-state β^- decay rate to the total β^- decay rate. This bound state decay channel leads to a definite reduction in the half-life of an atom in its highly ionized configurations. Moreover, the reduction factor (R) always exceeds unity for all three ionized states (He-like, H-like, and bare). However, it becomes the maximum for the bare atom. Additionally, our results show that bound-state decay dominates over continuum state decay for transitions with lower Q_n values. Furthermore, we observe that the lower the Q_n value, the larger the reduction factor.

These results may prove to be helpful in addressing the problems of nuclear waste management systems. Although achievable, it is highly challenging to produce these highly ionized and bare atoms terrestrially, hence the next step would be to focus on simulation-based work to analyse the energy expense and the effectiveness of these processes.

References

[1] Kenneth S. Krane, *Introductory Nuclear Physics* (John Wiley and Sons, Inc. , United States of America, 1998) 272-292

[2] Dr. S.N. Ghoshal, *Nuclear Physics* (S.Chand and Company ltd. Inc., India, 2021) 102-149

[3] A. Gupta, C. Lahiri, and S. Sarkar, Bound and continuum state β^- decay of bare atoms: Enhancement of decay rate and changes in β^- decay branching, Phys. Rev. C **100**, 064313 (2019). https://doi.org/10.1103/PhysRevC.100.064313

[4] R. Daudel, M. Jean and M. Lecoin, J. Phys. Radium **8**, 238 (1947).

[5] J. N. Bahcall, Theory of Bound-State Beta Decay, Phys. Rev. **124**, 495 (1961). https://doi.org/10.1103/PhysRev.124.495

[6] K. Takahashi and K. Yokoi, Beta-decay rates of highly ionized heavy atoms in stellar interiors, At. Data Nucl. Data Tables **36**, 375 (1987). https://doi.org/10.1016/0092-640X(87)90010-6

[7] K. Takahashi, R. N. Boyd, G. J. Mathews, and K. Yokoi, Bound-state beta decay of highly ionized atoms, Phys. Rev. C **36**, 1522 (1987). https://doi.org/10.1103/PhysRevC.36.1522

[8] M. Jung *et al.*, First observation of bound-state β^- decay, Phys. Rev. Lett. **69**, 2164, (1992). https://doi.org/10.1103/PhysRevLett.69.2164

[9] F. Bosch *et al.*, Observation of Bound-State β^- Decay of Fully Ionized ^{187}Re : ^{187}Re - ^{187}Os Cosmochronometry, Phys. Rev. Lett. **77**, 5190, (1996). https://doi.org/10.1103/PhysRevLett.77.5190

[10] A. Gupta, C. Lahiri, and S. Sarkar, Allowed β^- decay of bare atoms with A $\approx$ 60 - 80 in stellar environments, Phys. Rev. C **108**, 015805 (2023). https://dx.doi.org/10.1103/PhysRevC.108.015805

[11] R. S. Sidhu *et al.*, Measurement of the bound-state beta decay of bare $^{205}Tl^{+}_{81}$ ions at the ESR, EPJ Web of Conferences **279**, 06010, (2023). https://doi.org/10.1051/epjconf/202327906010

[12] K. Volanis, *A Theoretical Study on the Half-life of Bound-State Beta Decay (BSBD) of Long-Lived Fission Products*, Dissertation, KTH, 2024. https://urn.kb.se/resolve?urn=urn:nbn:se:kth:diva-352137.

[13] M. Joyce, Chapter 15 - Radioactive Waste Management and Disposal, Nuclear Engineering, 357 (2018). https://doi.org/10.1016/B978-0-08-100962-8.00015-9.

[14] H. Zerriffi and A. Makhijani, The Nuclear Alchemy Gamble An Assessment of Transmutation as a Nuclear Waste Management Strategy, (2005). https://ieer.org/resource/reports/nuclear-alchemy-gamble/

[15] A.B. Arslan, I. Yilmaz, G. Bakir, and H. Yapici, Transmutations of Long-Lived and Medium-Lived Fission Products Extracted from CANDU and PWR Spent Fuels in an Accelerator-Driven System, Science and Technology of Nuclear Installations, **2019**, 4930274, 13, (2019). http://dx.doi.org/10.1155/2019/4930274

[16] T. Wakabayashi, Y. Tachi, M. Takahashi, Study on method to achieve high transmutation of LLFP using fast reactor, Sci Rep **9**, 19156 (2019). https://doi.org/10.1038/s41598-019-55489-w

[17] National Nuclear Data Centre: NNDC, https://www.nndc.bnl.gov/nudat3/

[18] Atomic Spectra Database, https://physics.nist.gov/PhysRefData/ASD/ionEnergy.html

[19] K. Takahashi and K. Yokoi, Nucl. Phys. A **404**, 578 (1983). https://doi.org/10.1016/0375-9474(83)90277-4

[20] Hans. A. Bethe and Edwin E. Salpeter, *Quantum mechanics of one and two electron atoms* (Academic Press Inc., Germany, 1957) 63-70

[21] F. Salvat, J. M. Fernandez-Verea, and W. Williamson. Jr., Accurate numerical solution of the radial Schrödinger and Dirac wave equations, Phys. Commun. **90**, 151, (1995). https://doi.org/10.1016/0010-4655(95)00039-I

[22] F. Salvat and J. M. Fernandez-Verea, RADIAL: A Fortran subroutine package for the solution of the radial Schrödinger and Dirac wave equations, Phys. Commun. **240**, 165, (2019). https://doi.org/10.1016/j.cpc.2019.02.011

[23] B.H. Bransden and C.J. Joachain, *Physics of atoms and molecules* (John Wiley and Sons, Inc., Hong kong, 1990) 263-319

[24] J. C. Slater, Atomic Shielding Constants, Phys. Rev. **36**, 57, (1930). https://doi.org/10.1103/PhysRev.36.57

[25] E. J Konopinski and G. E. Uhlenbeck, On the Fermi Theory of β^- Radioactivity. II. The "Forbidden" Spectra, Phys. Rev. **60**, 308 (1941). https://doi.org/10.1103/PhysRev.60.308

[26] N.B. Gove and M.J. Martin, Log-f tables for beta decay, At. Data Nucl. Data Tables **10**, 205 (1971). https://doi.org/10.1016/S0092-640X(71)80026-8